Supermolecular structure of the enteropathogenic *Escherichia coli* type III secretion system and its direct interaction with the EspA-sheath-like structure

Kachiko Sekiya*†, Minako Ohishi†‡§¶, Tomoaki Ogino§¶, Koichi Tamano‖, Chihiro Sasakawa‖, and Akio Abe§¶**

*Laboratory of Electron Microscopy, School of Pharmaceutical Sciences, and §Laboratory of Bacterial Infection, Kitasato Institute for Life Sciences, Kitasato University, 5-9-1 Shirokane, Minato-ku, Tokyo 108-8641, Japan; ¶The Kitasato Institute, 5-9-1 Shirokane, Minato-ku, Tokyo 108-8642, Japan; and ‖Department of Microbiology and Immunology, Institute of Medical Science, University of Tokyo, 4-6-1 Shirokanedai, Minato-ku, Tokyo 108-8639, Japan

Communicated by Satoshi Omura, The Kitasato Institute, Tokyo, Japan, July 23, 2001 (received for review June 20, 2001)

Enteropathogenic *Escherichia coli* (EPEC) secretes several Esp proteins via the type III secretion system (secreton). EspA, EspB, and EspD are required for translocation of the effector proteins into host cells, in which EspB and EspD are thought to form a pore in the host membrane. Recent study has shown that EspA forms a filamentous structure that assembles as a physical bridge between bacteria and host cell surfaces, which then functions as a conduit for the translocation of bacterial effectors into host cells. To investigate the supermolecular structure of the type III secreton in EPEC, we partially purified it from the bacteria membrane and observed it via transmission electron microscopy. The EPEC type III secreton was composed of a basal body and a needle part and was similar to those of *Salmonella* and *Shigella*, except for a sheath-like structure at the tip of the needle. The length of sheath-like structures varied; it extended more than 600 nm and was 10 times longer than the *Shigella* needle part. The putative major needle component, EscF, was required for both secretion of Esp proteins and needle complex formation. Interestingly, elongation of the sheath-like structure was observed under constitutive expression of EspA but not of EscF. Furthermore, the transmission electron microscopy view with immunogold labeled anti-EspA antibodies clearly showed that EspA is a component of the sheath-like structure. This study revealed, to our knowledge for the first time, the supermolecular structure of the EPEC type III secreton and its direct association with the EspA-sheath-like structure.

Enteropathogenic *Escherichia coli* (EPEC) is a major cause of diarrhea in young children (1). Related pathogens, which cause disease by using similar mechanisms (2), include enterohemorrhagic *E. coli* O157:H7, rabbit enteropathogenic *E. coli*, and *Citrobacter rodentium*, which is found in mice. These pathogens induce a characteristic histopathological lesion, termed an attaching/effacing (A/E) lesion, which is defined by the intimate attachment of bacteria to the epithelial surface and the effacement of host cell microvilli (3). The A/E lesion is mediated by bacteria–host cell interactions, including triggering of host signal transduction pathways and cytoskeletal arrangements (4), and is required for full virulence *in vivo* (5).

Factors responsible for the A/E lesion formation are encoded by a 35-kilobase pair (kbp) locus termed the LEE (6), which encodes (*i*) the type III secretion system (the secreton) (7), (*ii*) the translocated intimin receptor (Tir) (8) and intimin (9), and (*iii*) Esp proteins. To elicit A/E lesion formation, Tir must be translocated into the host cell membrane via the type III secreton, and then the bacteria adhesion molecule, intimin, directly associates with the translocated Tir (8). Tir–intimin interaction is required for A/E lesion formation and induces accumulations of actin and other cytoskeletal components beneath the attached bacteria (8).

In addition to Tir, three other additional secreted proteins, EspA, EspB, and EspD, are required for formation of A/E lesions and are secreted via the EPEC/enterohemorrhagic *E. coli* type III secreton. EspA is a structural protein and the major component of a filamentous surface organelle termed "EspA filament" (10). The EspA filament forms a physical bridge between bacteria and the host cell, and it then functions as a conduit for the translocation of bacterial effectors into the host cell. EspB and EspD are thought to be delivered to the host cell membrane, and both proteins showed homology to *Yersinia* YopB/D proteins, which are believed to form a pore complex in the host membrane and correlate with the ability to induce contact-dependent hemolysis of red blood cells (RBCs) (11, 12). Recent study has shown that EPEC induces contact-independent hemolysis to RBCs, and EspA filament and EspD are required for this event (13, 14). On the other hand, the *espB* mutant still caused weak hemolysis, indicating that EspD may be the major component of a translocation pore into the host cell membrane (14). However, the contradictory finding has been presented that the *espB* mutant showed the nonhemolytic phenotype (13).

Type III secretons are found in many other Gram-negative bacteria species, and they are the mechanism for translocation of bacterial proteins into host cells. Many components of type III secretons show sequence similarities with those of flagellar basal bodies (15). Kubori *et al.* identified the supermolecular structure termed the "needle complex" (NC) from the *Salmonella* type III secreton (16), and a similar structure was also identified from *Shigella* (17, 18), indicating that the type III secreton appears to have universal form. The size of each part of the *Shigella* NC has been characterized and measured (17); the needle part is 8 nm wide and 45 nm long, and the basal body consists of upper and lower doublet rings with diameters of 15 and 26 nm, respectively, and resembles those of flagella. The height of the basal body is 32 nm, which presumably allows it to traverse both bacterial membranes and the peptidoglycan. The protein components of the NC have been proposed and characterized in both *Salmonella* (16, 19, 20) and *Shigella* (17, 18). These studies have revealed that in *Salmonella*, the basal body is composed of PrgH/K and InvG, and the needle part is composed of PrgI/J. In *Shigella*, the basal body and needle part are composed of MxiD/G/J and MxiH/I. MxiG, MxiJ, MxiD, MxiH, and MxiI

Abbreviations: EPEC, enteropathogenic *E. coli*; NC, needle complex; TEM, transmission electron microscopy; WT, wild type; Tir, translocated intimin receptor; A/E, attaching/effacing.

†K.S. and M.O. contributed equally to this work.

‡Present address: Department of Molecular and Cellular Biology, Research Institute for Microbial Disease, Osaka University, 3-1 Yamadaoka, Suita, Osaka 565-0871, Japan.

**To whom reprint requests should be addressed. E-mail: akioabe@kitasato-u.ac.jp.

The publication costs of this article were defrayed in part by page charge payment. This article must therefore be hereby marked "*advertisement*" in accordance with 18 U.S.C. §1734 solely to indicate this fact.

 www.pnas.org/cgi/doi/10.1073/pnas.191378598

show sequence similarity to PrgH, PrgK, InvG, PrgI, and PrgJ, respectively.

Although extensive knowledge has been accumulated about the EPEC type III secreton and EspA filament, the supermolecular structure of the type III secreton and its relationship to EspA filament are poorly understood. Interestingly, no EspA homologue was found in components of type III secretons in *Salmonella*, *Shigella*, and other pathogens, except for enterohemorrhagic *E. coli*. In the EspA defect strain, EspB and EspD are still secreted into the culture supernatant (21), but they are not able to translocate both proteins into host cells (10, 14), suggesting that the assembly of the EPEC type III secreton may be somewhat different from those of *Salmonella* or *Shigella*, and that EspA may be associated with the type III secreton. We report here the identification and characterization of the EPEC type III secreton and its relationship to EspA.

Materials and Methods

Bacterial Strains and Growth Media. EPEC was grown in LB broth or DMEM at 37°C. *Shigella* was grown in LB broth at 37°C. For details of strains and its phenotypes, see Table 1, which is published as supporting information on the PNAS web site, www.pnas.org.

Cloning and Construction of the Nonpolar Mutant. EPEC *escF* and *espA* were cloned into pTrc99A (Amersham Pharmacia) to obtain p99-*escF*s and p99-*espA*, which constitutively produce EspA and EscF and which were used for complementation of *espA* and *escF* mutants. Details of clones and construction of EPEC Δ*escF* (strain KILS001) can be found in the supporting *Methods*, which are published on the PNAS web site.

Purification of the NCs from EPEC and *Shigella*. EPEC and its mutant strains were grown in LB broth overnight at 37°C without shaking, and then overnight cultures were diluted 1:25 in DMEM and incubated for 5 h in a CO_2 incubator. *Shigella* or EPEC was grown in LB broth overnight at 37°C with shaking, and then overnight culture was diluted 1:100 in LB broth and incubated for 2.5 h at 37°C with shaking. Bacteria were then harvested, and the NC was purified by protocols for the partial purification of the *Shigella* NC (17).

Preparation of Secreted Proteins, SDS/PAGE, and Immunoblotting. Bacteria grown in DMEM or LB were removed by centrifugation (18,000 × *g*, 10 min), and proteins in the supernatant were precipitated by the addition of ice-cold trichloroacetic acid at a final concentration of 10% and then incubated on ice for 1 h. After centrifugation, the pellets were resuspended in Laemmli sample buffer and analyzed by SDS/PAGE. For immunoblotting, the proteins were resolved by SDS/PAGE and transferred to polyvinylidene difluoride membranes. EspA, EspB, and EscC were detected with guinea pig polyclonal antibodies against their respective recombinant proteins. Antibodies were purified by affinity chromatography by using respective antigen-immobilized columns.

Infection of Cultured Cells and Immunofluorescence Microscopy. HeLa cells (10^5) were seeded and grown overnight on 12-mm round glass coverslips, then infected with bacteria for 3 h. Cells were washed three times with PBS and fixed with 3.0% paraformaldehyde in PBS (pH 7.2), then washed three times with PBS. The fixed cells were permeabilized with 20 μl 0.1% Triton X-100 in PBS in the presence of phalloidin–Texas red (to stain filamentous actin) or antiphosphotyrosine antibodies (4G10, Upstate Biotechnology). Alexa-conjugated anti-mouse IgG and IgM (Molecular Probes) were used as the secondary antibody for antiphosphotyrosine. Stained samples were visualized and photographed as described elsewhere (22).

Hemolysis Assay. Bacteria were grown in LB broth overnight at 37°C without shaking, and then overnight cultures were diluted 1:25 into DMEM and incubated for 4 h in a CO_2 incubator. They were collected by centrifugation and resuspended in fresh DMEM corresponding to 1/10 volume of the culture media. Rabbit blood cells (RBCs) were sedimented, washed three times in PBS, and resuspended with DMEM at 10^9/ml. Equal volumes of bacteria and RBC suspension were mixed together, and each 100-μl aliquot was poured into round-bottom 96-well plates and incubated at 37°C for 90 min in the CO_2 incubator. The bacteria–RBC suspensions were gently resuspended with an additional 150 μl of PBS, and then plates were centrifuged. Supernatants (100 μl) were transferred to a fresh plate, where optical density at 550 nm was measured.

Electron Microscopy. Samples were negatively stained with 2% phosphotungstic acid, pH 7.3, that contained 0.2% (wt/vol) sucrose on Butval-98 grids and observed under a JEM 1010 transmission electron microscope (JEOL). For immunolabeling of the NC, samples were applied to Butval-98 grids, fixed with 1% formaldehyde in physiological salt solution, immunolabeled with the affinity-purified anti-EspA polyclonal antibody and with 6-nm colloidal gold-conjugated antibodies against guinea pig IgG (Aurion, Wageningen, The Netherlands) at room temperature for 20 min. After further thorough washing, the NC were fixed and stained as described above.

Results and Discussion

Supermolecular Structure of the EPEC Type III Secreton. To identify the supermolecular structure of the EPEC type III secreton, EPEC was grown in LB broth, and the NC fraction was prepared, negatively stained, and then observed by transmission electron microscopy (TEM). Although we could detect a supermolecular structure similar to that of the *Shigella* NC, the major components were flagella complexes (Fig. 1*A*). It has been reported that expression of Esp proteins is affected by environmental conditions such as culture media (23), host body temperature (24), and Congo red (25). Indeed, expression of Esp proteins was induced when EPEC was grown in DMEM but not in LB broth (Fig. 3*C*). Therefore, the NC fraction was prepared from EPEC wild type (WT) grown in DMEM and observed by TEM (Fig. 1*B*). On induction in DMEM, the number of flagella complexes was greatly reduced, and the number of NCs with cylindrical symmetry was predominantly increased (white arrow in Fig. 1*B*). Although the basal body of the NC was reminiscent of that of *Shigella* (arrows in Fig. 1*D*), the needle was extraordinarily long and thick (Fig. 1*B*). To exclude the possibility that the long needle may be specific to the E2348/69 strain (serotype O127), NCs were also prepared from B171–8 (serotype O111) and rabbit enteropathogenic *E. coli* (REPEC) (serotype O103) strains (Fig. 1*C* and summarized in Table 1). The TEM view clearly showed that NCs from B171–8 and REPEC had the same shape as that of E2348/69. Our preparation techniques were also confirmed by using *Shigella flexneri* M94 strain (17), and we found the typical *Shigella* NCs (arrows in Fig. 1*D*) that had already been characterized elsewhere (17, 18). To further characterize the needle parts, TEM images of 13 particles were aligned, and these structures were compared with those of *Shigella* (Fig. 1*E*). In contrast to *Shigella*, the length of the needle varied, and some of the needles were more than 600 nm long (Fig. 1*E*). Needle elongation has not been observed in *Shigella* WT, unless the major needle component, MxiH, was overexpressed (17). In this study, we also observed pilus-like structures from different serotypes of EPEC (black arrows in Fig. 1 *B* and *C*), and these structures were not observed in *Shigella* NC fraction (Fig. 1*D*), indicating that EPEC possesses additional surface appendages that were different from NCs.

EPEC drastically changed the supermolecular structure on the

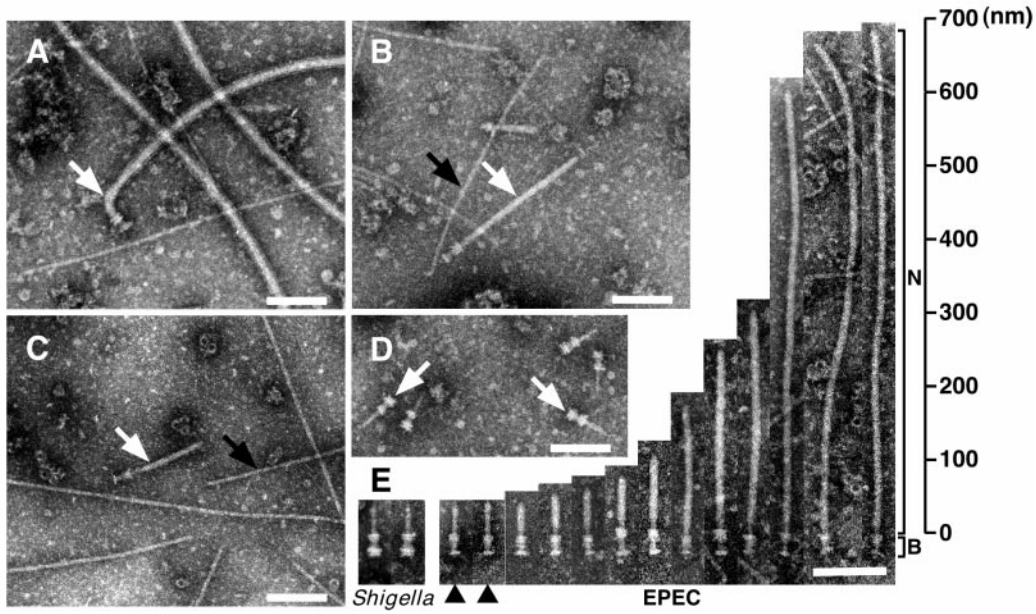

Fig. 1. Electron micrographs of negatively stained NC fractions from EPEC and *Shigella*. The NCs were partially purified from EPEC E2348/69 strain grown in LB broth (*A*), in DMEM (*B*), and from EPEC B171–8 grown in DMEM (*C*). (*D*) Electron micrograph of purified *Shigella* NC. (*E*) Alignment of EPEC NCs and comparisons to *Shigella*. N and B indicate the needle and basal body of EPEC NCs, respectively. Black arrowheads indicate putative immature NCs. White arrows indicate flagellar complexes (*A*) and NCs (*B*, *C*, and *D*). Black arrows indicate pilus-like structures. (Bars = 100 nm.)

bacterial cell surface when the environmental condition was shifted to an *in vivo* conditional medium such as DMEM from an *in vitro* rich medium such as LB media (Fig. 1 *A* and *B*). These observations may indicate that EPEC has two different phases: (*i*) a planktonic phase where the flagella complex is used to aid in bacterial swimming; and (*ii*) a virulent phase where the production of flagella complexes is repressed, and instead the type III secreton is produced to use for the translocation of bacterial effectors into the host cells.

EscF Is Required for A/E Lesion Formation, Hemolytic Activity, and Secretion. To investigate whether the NC was an EPEC type III secreton, we decided to disrupt a gene encoding EscF. EscF showed homology to the major needle parts of type III secretons in *S. typhimurium* SPI1 PrgI (24% identity) (19) and *Shigella flexneri* MxiH (25% identity) (17). In addition, EscF shared homology with other putative type III needle parts of *S. typhimurium* SPI2 SsaH (35% identity), *Pseudomonas aeruginosa* PscF (25% identity) (Fig. 2*A*). The *escF* located on the *LEE4* transcriptional unit in EPEC LEE (26, 27) (Fig. 2*C*) was amplified by PCR, and the *escF* mutant strain was constructed as described in the supporting *Methods*. To analyze whether EscF is involved in A/E lesion formation, HeLa epithelial cells were infected with WT and Δ*escF*, and then cytoskeletal actin and phosphorylated proteins were labeled with phalloidin–Texas red and fluorescently labeled antiphosphotyrosine antibody, respectively (Fig. 3*A*). Infection with WT induced the accumulation of actin and tyrosine-phosphorylated proteins beneath the adherent bacteria. In contrast, infection with the *escF* mutant did not elicit A/E lesion formation. Complementation of Δ*escF* with the cloned *escF in trans* restored the ability to form A/E lesions. These results indicate that the lack of cytoskeletal rearrangements could be attributed to the disruption of *escF*.

A recent study showed that EPEC induces contact-independent hemolysis in RBCs, and that this hemolytic activity depends on the type III secreton (14). To confirm the contribution of EscF to the EPEC-induced hemolysis, we measured the hemolytic activity of the *escF* mutant and compared its activity

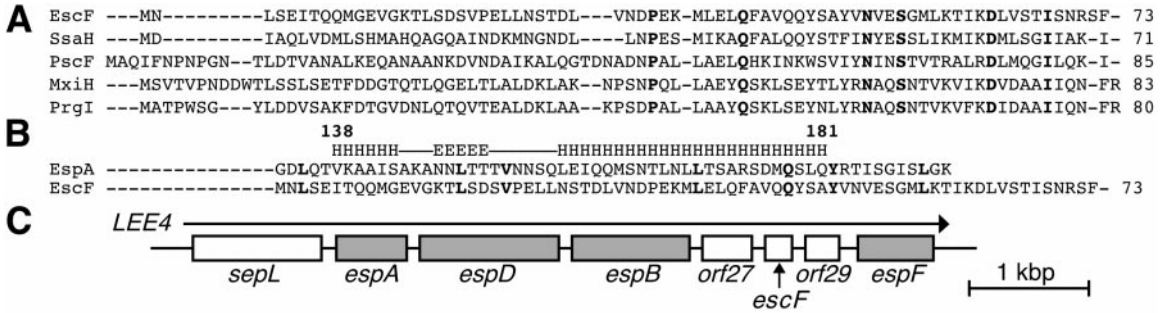

Fig. 2. Sequence analyses of EscF and EspA and a genetic map of the *LEE4*. (*A*) The sequence analyses of needle parts were performed with BLAST (National Center for Biotechnology Information, http://www.ncbi.nlm.nih.gov/). (*B*) The N terminus of EscF showed homology (13% identity) to the C terminus of EspA (135–190 aa) that contains the coiled-coil region (138–181 aa). The EspA coiled-coil region predicted elsewhere (30) is illustrated (E, β sheet; H, α helix). Note that the leucine-rich heptad repeat of EscF at position Leu^{3}-Leu^{38} was overlapped with the heptad repeat in EspA coiled-coil region that is required for the A/E lesion formation and EspA-EspA interaction (30). Bold letters indicate identical amino acids. (*C*) Organization of *esp* genes and *escF* in the *LEE4* transcriptional unit. An arrow indicates the direction of transcription, and gray boxes indicate genes encoding secreted proteins.

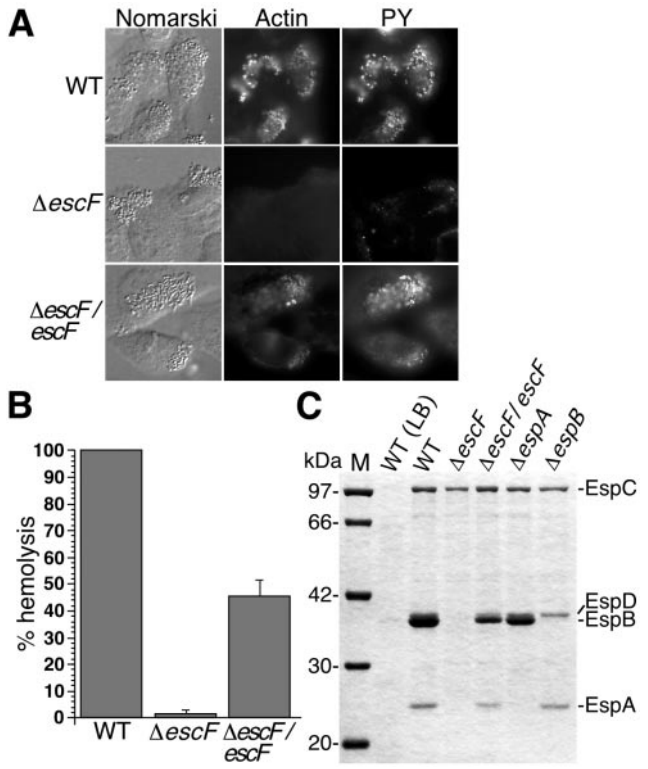

Fig. 3. The effect of *escF* mutation on A/E lesion formation, hemolytic activity, and secretion of Esp proteins. (*A*) Infected HeLa cells with WT or *escF* mutant were fixed, and then actin and tyrosine-phosphorylated proteins (PY) were detected by immunofluorescence microscopy. (*B*) Contact-independent hemolytic activity. EPEC WT and the *escF* mutant strains were assayed for their ability to hemolyze RBCs. Results from three independent experiments are shown. Error bars, standard deviation. (*C*) Secreted protein profiles of EPEC WT and *escF* mutant strains. Bacteria were grown in DMEM or LB broth, and secreted proteins were resolved by 10% SDS/PAGE and stained with Coomassie blue.

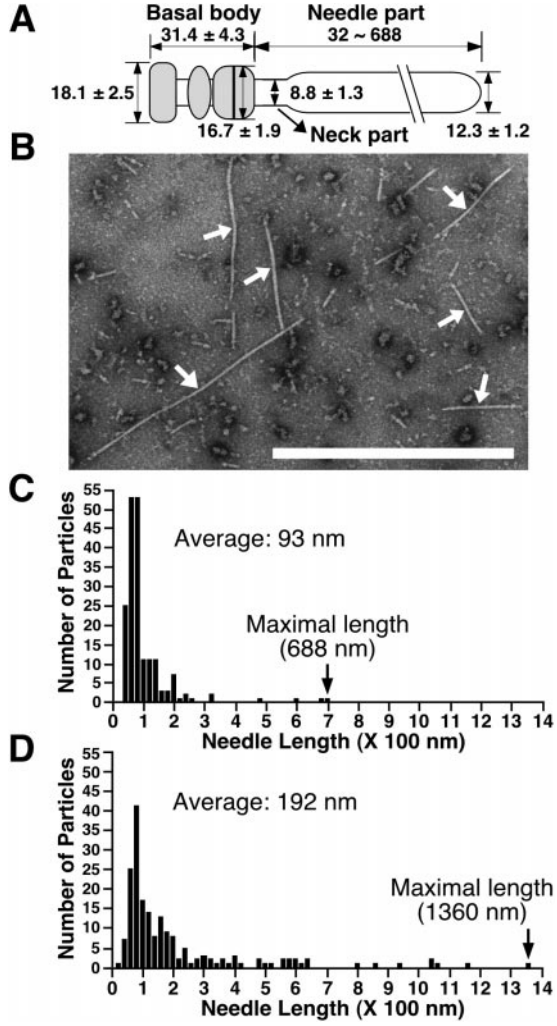

Fig. 4. (*A*) Presumed model of the EPEC NC with the sheath-like structure. Each size is represented in nanometers. The gray area indicates the basal body. (*B*) Electron micrographs of the negatively stained NC prepared from the *espA* mutant containing cloned *espA*. Arrows indicate NCs. (Bar = 1 μm.) Distribution of the needle length in the NCs purified from EPEC WT (*C*) and the *espA* mutant containing *espA* (*D*).

to that of WT (Fig. 3*B*). Hemolytic activity was observed in WT without close contact to RBCs by centrifugation. In contrast, this activity was completely abolished by the *escF* mutant, and it was partially restored when cloned *escF* was reintroduced into the *escF* mutant *in trans*, indicating that EscF is involved in the hemolysis. *Yersinia* (11, 12) and *Shigella* (28, 29) induce hemolytic activities, but centrifugation is required for to evoke hemolysis in RBCs. These findings indicate that the contact-independent hemolysis in EPEC infection can probably be attributed to the extraordinary length of the needle indicating the formation of an EspA filament (10). Indeed, EPEC needle parts varied and were longer than those of *Shigella* (Fig. 1*E*), thus permitting the elongated needle to be in direct contact with RBCs without centrifugation.

To further investigate the defect caused by *escF* mutation, EPEC-secreted proteins were analyzed by 12% SDS/PAGE. As shown in Fig. 3*C*, secretion of EspA, EspB, and EspD was completely blocked by the *escF* mutation. Complementation of the *escF* mutant with cloned *escF in trans* restored secretion of all type III secreted proteins. These results indicate that EscF is required for the secretion of Esp proteins, and this observation agrees with secretion-defect phenotypes of mutant strains of *Shigella mxiH* (17, 18) and *Salmonella prgI* (19, 20) that encode major needle components.

Characterization and Assembly of the EPEC NC. We prepared and measured 34 conserved NCs from EPEC WT, and each part was estimated, as shown in Fig. 4*A*. Although we could not figure out exact sizes of lower and upper rings of the basal body because of the instability in the structure, both rings appeared to be doublet. The widths of the upper and lower rings were estimated to be 16.7 ± 1.9 and 18.1 ± 2.5 nm, respectively, and the height of the basal body was 31.4 ± 4.3 nm. These observations indicate that diameters of the upper and lower rings in EPEC type III secretons are somewhat smaller than those of *Shigella* (Fig. 1*E*), whereas the height of the EPEC basal body is nearly identical to that of *Shigella*. In contrast to *Shigella* and *Salmonella*, the EPEC needle is associated with unknown components that seemed to form a sheath-like structure (12.3 ± 1.2 nm in width, Fig. 1*E*). The measured value was wider than the width of the *Shigella* needle [8.0–8.5 nm; Tamano *et al.* (17) and this study]. Furthermore, minor particles, less than 1% of the total particles, of EPEC NCs appear to have thinner needles (arrowheads in Fig. 1*E*). Indeed, the NCs possessing the thin needles (termed the neck part in this study), which were located between the sheath-like structure and the basal body, are similar in widths to those of *Shigella*. These findings suggest that the sheath-like structure is associated with the surface of the needle part and that the needle structure is extended from the basal body of the EPEC type III secreton.

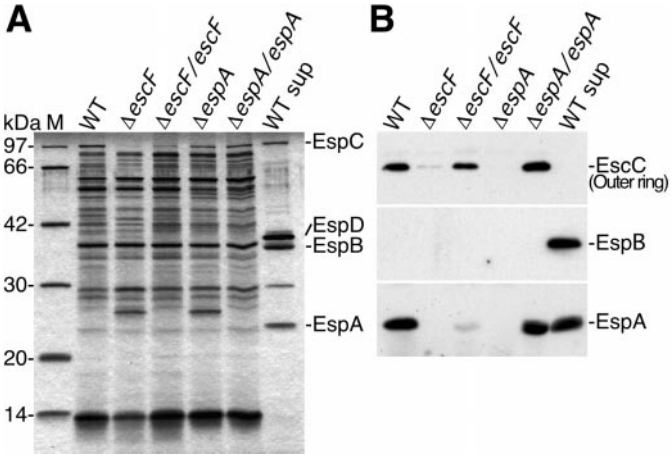

Fig. 5. The effect of *escF* and *espA* mutations on the NC formation. (*A*) NC fractions were prepared and analyzed by 12% SDS/PAGE followed by silver staining. (*B*) Immunoblot analysis of NC fractions from EPEC WT and its mutants. Affinity-purified anti-EspA, -EspB, and -EscC antibodies were used for immunodetection. M and WT sup indicate the size marker and secreted proteins prepared from the EPEC WT, respectively.

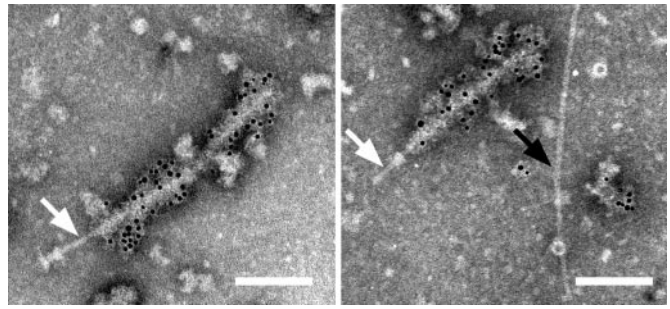

Fig. 6. Direct association of EPEC type III secreton with EspA. The NC was partially purified from EPEC WT, and EspA was detected with the immunogold-labeled anti-EspA antibodies. Sheath-like structures coated with 6-nm gold particles were observed. Note that the neck (white arrow, *Left*), the stem beneath the upper ring (white arrow, *Right*), and the pilus-like structure (black arrow, *Right*) were not stained with the anti-EspA antibodies.

Next, we prepared NCs from various mutants and observed them by TEM (summarized in Table 1). As expected, the *espB* mutant did not affect the NC formation. In contrast, NCs were not detected in the type III secretion-defective strain, CVD452 (*escN* mutant strain). As in the case of CVD452, NCs were not detected in the *escF* mutant, but NCs were restored when cloned *escF* was reintroduced into the *escF* mutant *in trans*. Although the *Shigella* needle was elongated up to 1 μm when MxiH was overexpressed, we did not observe needle elongation in the *escF* mutant containing cloned *escF,* which allows constitutive expression (data not shown). Interestingly, the NC formation was completely abolished by the *espA* mutant; even secretion of EspB and EspD was not affected by this mutation (Fig. 3*C*). In contrast, the NC was completely restored when cloned *espA* was introduced into the *espA* mutant *in trans*. To our surprise, the sheath-like structure in this strain appears to be longer than that of the EPEC WT (Fig. 4*B*). To confirm this observation, we examined the distribution of needle length in 187 randomly chosen NCs from WT (Fig. 4*C*) and Δ*espA* containing cloned *espA* (Fig. 4*D*). Needle lengths of WT varied, ranging from 32 to 688 nm (average, 93 nm) with a peak at 40–140 nm. Although the peak of the needle length in Δ*espA* containing cloned *espA* was similar to that of WT, the needle length was distributed over a wider range, from 32 to 1,360 nm (average, 192 nm), with the maximal size nearly corresponding to the whole bacterial size. For complementation studies of *escF* and *espA* mutants, we used the same expression vector and growth conditions. We determined that EspA, but not EscF, may be a major component of the sheath-like structure, because the length of the sheath-like structure appears to be controlled by the amount of EspA.

Component of the NC with the Sheath-Like Structure. To further analyze the requirement of EspA for NC formation, we analyzed NC fractions by silver staining 12% SDS/PAGE (Fig. 5*A*). The NC fraction prepared from WT, Δ*escF*, and Δ*espA* appears to contain other components, because unknown pilus-like structures were also observed in this NC fraction (Fig. 1*B*), and we could not detect drastic changes of NC fractions between WT and mutants. Next, EspA was detected by immunoblotting by using anti-EspA antibodies. Although we detect EspA in the bacterial culture supernatant (Fig. 3*C*), we also detected it in the NC fraction prepared from WT (Fig. 5*B*). To eliminate the possibility of contamination of bacterial culture supernatants into the NC fraction, immunoblotting was carried out by using antibodies against EspB secreted into culture supernatants. As expected, EspB was not detected in the NC fraction. These results indicate that EspA is specifically localized in the NC fraction. Furthermore, EspA was not detected in the NC fraction prepared from the *escF* mutant, and the localization of EspA in the NC fraction was partially restored by reintroduction of cloned *escF* into the *escF* mutant *in trans*, indicating that the EspA may be associated with EscF.

Although basal bodies, type III secretons without needles, have been observed in *Shigella mxiH* (17, 29) and *Salmonella prgI* (20) mutants, we could not detect basal body structure in *escF* and *espA* mutants. To analyze the basal body, we tried to detect EscC by immunoblotting (Fig. 5*B*). EscC is thought to be one of components of the basal body and showed homology to the *Shigella* MxiD outer ring. Although EscC was detected in the NC fraction from WT, this protein was greatly decreased in both of the *escF* and *espA* mutants, and even MxiD has been detected in the NC prepared from the *mxiH* mutant (17). Both deficient phenotypes were restored in the reintroduction of cloned *escF* or *espA* into their respective strains. These results agreed with our TEM views and explained why we could not detect basal bodies from *escF* and *espA* mutants. Collectively, EscF and EspA may affect the assembly and stability of the basal body.

EspA Directly Associates with the NC and Is an Essential Component of the Sheath-Like Structure. The study cited above suggests that EspA may interact directly with the type III secreton. To confirm this fascinating hypothesis, NCs purified from EPEC WT were stained with immunogold-labeled anti-EspA antibodies and observed by TEM (Fig. 6). The TEM view clearly showed that the sheath-like structure was attached to the tip of the needle part (an arrow in the left column), and the needle beyond the upper ring is observed from the incomplete NC lacking the lower base (an arrow in the right column). To our surprise, only the sheath-like structure was stained with the anti-EspA antibodies. In contrast, the needle, which was observed as the neck part (Fig. 1*E* and an arrow in the left column in Fig. 6), and the needle beneath the upper ring (an arrow in the right column in Fig. 6) were not labeled with anti-EspA antibodies. Our TEM view was strongly supported by the finding of Shaw *et al.* (14), who showed that about 50 nm of the EspA filament close to the bacterial surface was not stained with anti-EspA antibodies. Although we observed an unknown pilus-like structure (black arrow in Fig. 6; Fig. 1 *B* and *C*), this did not react to the anti-EspA antibodies. These results clearly indicate that EspA is the major component of the sheath-like structure, which is supported by elongation of the sheath-like structure under constitutive expression of EspA (Fig. 4*B*).

In conclusion, we have shown, to our knowledge for the first time, a direct association of the EPEC type III secreton with EspA. A hypothetical model of the EPEC type III secreton and the sheath-like structure is illustrated in Fig. 7. First, the inner and outer ring components are assembled; a *sec*-dependent pathway probably requires this step, because the typical signal peptide exists in the outer ring component, EscC. Second, EscF is polymerized and assembled into outer and inner rings, and then EspA is secreted via the type III secreton and attached to the tip of the needle. Recently, Delahay *et al.* revealed that a coiled-coil domain with heptad periodicity is located at the C terminus of EspA (Fig. 2*B*) (30), and that this domain is required for EspA–EspA interaction. Interestingly, we found that the N terminus of EscF showed homology to the coiled-coil domain of EspA (Fig. 2*B*). Probable interaction between the EspA-coiled-coil domain and EscF helps the stability of the type III secreton, because the NC was not detected in the *espA* mutant. Finally, EspA initiates the polymerization from the tip of the needle and assembles the sheath-like structures. The sheath-like structure is expandable, and its elongation is controlled by the amount of EspA (Fig. 4*B*). The sheath-like structure builds a physical bridge between the bacterium and the host cell membrane, and Tir and other effectors can translocate into host cells.

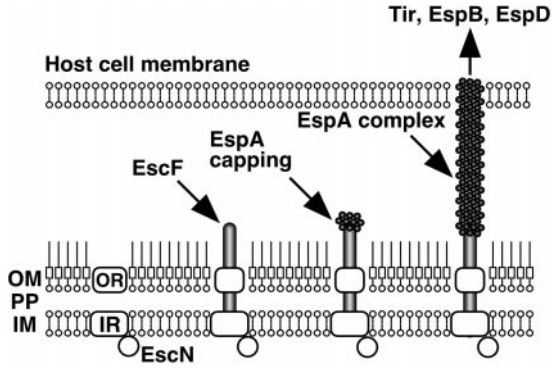

Fig. 7. Schematic model of the assembly of the EPEC type III secreton and the sheath-like structure. First, inner and outer ring components are assembled, and then EscF is polymerized and assembled into the outer and inner rings. EspA is secreted via the type III secreton and attached to the tip of the needle. Finally, EspA initiates the polymerization and assembles the sheath-like structure. The sheath-like structure is expandable and is controlled by the amount of EspA (Fig. 4*B*). The sheath-like structure builds a physical bridge between the bacterium and the host cell membrane, and Tir and other effectors can be translocated into host cells. OM, outer membrane; PP, periplasm; IM, inner membrane; OR, outer ring; IR, inner ring.

MICROBIOLOGY

We thank Brett Finlay (Biotechnology Laboratory, University of British Columbia, Vancouver, BC, Canada), Jim Kaper (Center for Vaccine Development and Department of Microbiology and Immunology, University of Maryland School of Medicine, Baltimore, MD), and Michael Donnenberg (Division of Infectious Diseases, Department of Medicine, University of Maryland School of Medicine, Baltimore, MD) for providing the E2348/69 derivatives. We also thank Asaomi Kuwae for critical reading for the manuscript and helpful discussions. This work was supported by operating grants from the Research for the Future Program of the Japanese Society for the Promotion of Science and the All Kitasato Project Study.

1. Donnenberg, M. S. & Kaper, J. B. (1992) *Infect. Immun.* **60,** 3953–3961.
2. DeVinney, R., Gauthier, A., Abe, A. & Finlay, B. B. (1999) *Cell. Mol. Life Sci.* **55,** 961–976.
3. Moon, H. W., Whipp, S. C., Argenzio, R. A., Levine, M. M. & Giannella, R. A. (1983) *Infect. Immun.* **41,** 1340–1351.
4. Rosenshine, I., Donnenberg, M. S., Kaper, J. B. & Finlay, B. B. (1992) *EMBO J.* **11,** 3551–3560.
5. Abe, A., Heczko, U., Hegele, R. G. & Finlay, B. B. (1998) *J. Exp. Med.* **188,** 1907–1916.
6. McDaniel, T. K., Jarvis, K. G., Donnenberg, M. S. & Kaper, J. B. (1995) *Proc. Natl. Acad. Sci. USA* **92,** 1664–1668.
7. Jarvis, K. G., Giron, J. A., Jerse, A. E., McDaniel, T. K., Donnenberg, M. S. & Kaper, J. B. (1995) *Proc. Natl. Acad. Sci. USA* **92,** 7996–8000.
8. Kenny, B., Devinney, R., Stein, M., Reinscheid, D. J., Frey, E. A. & Finlay, B. B. (1997) *Cell* **91,** 511–520.
9. Jerse, A. E., Yu, J., Tall, B. D. & Kaper, J. B. (1990) *Proc. Natl. Acad. Sci. USA* **87,** 7839–7843.
10. Knutton, S., Rosenshine, I., Pallen, M. J., Nisan, I., Neves, B. C., Bain, C., Wolff, C., Dougan, G. & Frankel, G. (1998) *EMBO J.* **17,** 2166–2176.
11. Hakansson, S., Schesser, K., Persson, C., Galyov, E. E., Rosqvist, R., Homble, F. & Wolf-Watz, H. (1996) *EMBO J.* **15,** 5812–5823.
12. Neyt, C. & Cornelis, G. R. (1999) *Mol. Microbiol.* **33,** 971–981.
13. Warawa, J., Finlay, B. B. & Kenny, B. (1999) *Infect. Immun.* **67,** 5538–5540.
14. Shaw, R. K., Daniell, S., Ebel, F., Frankel, G. & Knutton, S. (2001) *Cell Microbiol.* **3,** 213–222.
15. Hueck, C. J. (1998) *Microbiol. Mol. Biol. Rev.* **62,** 379–433.
16. Kubori, T., Matsushima, Y., Nakamura, D., Uralil, J., Lara-Tejero, M., Sukhan, A., Galan, J. E. & Aizawa, S. I. (1998) *Science* **280,** 602–605.
17. Tamano, K., Aizawa, S., Katayama, E., Nonaka, T., Imajoh-Ohmi, S., Kuwae, A., Nagai, S. & Sasakawa, C. (2000) *EMBO J.* **19,** 3876–3887.
18. Blocker, A., Jouihri, N., Larquet, E., Gounon, P., Ebel, F., Parsot, C., Sansonetti, P. & Allaoui, A. (2001) *Mol. Microbiol.* **39,** 652–663.
19. Kubori, T., Sukhan, A., Aizawa, S. I. & Galan, J. E. (2000) *Proc. Natl. Acad. Sci. USA* **97,** 10225–10230. (First Published August 15, 2000; 10.1073/pnas.170128997)
20. Kimbrough, T. G. & Miller, S. I. (2000) *Proc. Natl. Acad. Sci. USA* **97,** 11008–11013. (First Published September 12, 2000; 10.1073/pnas.200209497)
21. Kenny, B., Lai, L. C., Finlay, B. B. & Donnenberg, M. S. (1996) *Mol. Microbiol.* **20,** 313–323.
22. Finlay, B. B., Ruschkowski, S. & Dedhar, S. (1991) *J. Cell. Sci.* **99,** 283–296.
23. Kenny, B., Abe, A., Stein, M. & Finlay, B. B. (1997) *Infect. Immun.* **65,** 2606–2612.
24. Abe, A., Kenny, B., Stein, M. & Finlay, B. B. (1997) *Infect. Immun.* **65,** 3547–3555.
25. Abe, A. & Nagano, H. (2000) *Microbiol. Immunol.* **44,** 857–861.
26. Mellies, J. L., Elliott, S. J., Sperandio, V., Donnenberg, M. S. & Kaper, J. B. (1999) *Mol. Microbiol.* **33,** 296–306.
27. Friedberg, D., Umanski, T., Fang, Y. & Rosenshine, I. (1999) *Mol. Microbiol.* **34,** 941–952.
28. Sansonetti, P. J., Ryter, A., Clerc, P., Maurelli, A. T. & Mounier, J. (1986) *Infect. Immun.* **51,** 461–469.
29. Blocker, A., Gounon, P., Larquet, E., Niebuhr, K., Cabiaux, V., Parsot, C. & Sansonetti, P. (1999) *J. Cell. Biol.* **147,** 683–693.
30. Delahay, R. M., Knutton, S., Shaw, R. K., Hartland, E. L., Pallen, M. J. & Frankel, G. (1999) *J. Biol. Chem.* **274,** 35969–35974.